Systematics of Distributions of Various Elements Between Ferromanganese Oxides and Seawater from Natural Observation, Thermodynamics, and Structures

4

Yoshio Takahashi, Daisuke Ariga, Qiaohui Fan, and Teruhiko Kashiwabara

Abstract

Metal oxides including iron oxides, manganese oxides, and ferromanganese oxides have been frequently found at seafloor as a result of the release of dissolved iron and manganese from various sources including hydrothermal activities. These precipitates can adsorb or incorporate various elements, which can affect the behavior of the elements in marine environment. In addition, these precipitates can be resources of rare metals due to their high abundances in ferromanganese oxides. In this review, our aims are (i) to summarize distribution of various trace elements between ferromanganese oxides and seawater, (ii) to understand the distributions based on thermodynamic parameters, and (iii) to show the relationship between the distribution and structural information of the species adsorbed onto the ferromanganese oxides. For this purpose, our original data of chromate adsorption on ferrihydrite was also included. These attempts enable us to obtain systematic explanation of the solid-water distributions of various elements in marine environment, which in turn gives us clearer view on (i) the mechanism of isotopic fractionation during adsorption which is linked to the understanding of paleoenvironment based on the isotope geochemistry and (ii) prediction of abundances of various elements in the ferromanganese oxides that are important from the viewpoint of exploration of marine resources.

Keywords

Ferromanganese oxide • Adsorption • Surface complex • Systematics • EXAFS

Y. Takahashi (✉)
Department of Earth and Planetary Science, Graduate School of Science, The University of Tokyo, 7-3-1 Hongo, Bukyo-ku, Tokyo 113-0033, Japan

Department of Earth and Planetary Systems Science, Graduate School of Science, Hiroshima University, 1-3-1 Kagamiyama, Higashi-Hiroshima, Hiroshima 739-8526, Japan

Institute for Research on Earth Evolution(IFREE)/Submarine Resources Research Project (SRRP), Japan Agency for Marine-Earth Science and Technology (JAMSTEC), 2-15 Natsushimacho, Yokosuka, Kanagawa 237-0061, Japan
e-mail: ytakaha@eps.s.u-tokyo.ac.jp

D. Ariga • Q. Fan
Department of Earth and Planetary Systems Science, Graduate School of Science, Hiroshima University, 1-3-1 Kagamiyama, Higashi-Hiroshima, Hiroshima 739-8526, Japan

T. Kashiwabara
Institute for Research on Earth Evolution(IFREE)/Submarine Resources Research Project (SRRP), Japan Agency for Marine-Earth Science and Technology (JAMSTEC), 2-15 Natsushimacho, Yokosuka, Kanagawa 237-0061, Japan

J.-i. Ishibashi et al. (eds.), *Subseafloor Biosphere Linked to Hydrothermal Systems: TAIGA Concept*,
DOI 10.1007/978-4-431-54865-2_4,

4.1 Introduction

In natural waters, precipitation-dissolution process is primarily controlling the dissolved concentrations of various elements, especially for major elements at earth's surface such as calcium and iron. It is often the case, however, that concentrations of trace elements in seawater are controlled by the adsorption-desorption reactions between water and various solid phases such as particulate matters, chemical deposits, and sediments present in marine environment (Langmuir 1997). In particular, adsorption mechanism and local structure of ions adsorbed on the solid phases are closely related to their concentrations in the aqueous phase. Moreover, it has been recently revealed that isotopic ratios of trace elements in seawater were also affected by the adsorption-desorption reactions (Lyons et al. 2009; Kashiwabara et al. 2011). Among various phases, iron and manganese oxides play an important role on controlling concentrations and isotopic ratios of trace elements in seawater.

In marine environment, metal ions are supplied mainly from fluvial source, hydrothermal fluid at seafloor vent, and dissolution of airborne particles at seawater surface. Among them, it has been indicated that the amounts of iron and manganese supplied from hydrothermal activities to ocean are larger than those from fluvial components as a total budget (Elderfield and Schultz 1996). Although it has been shown that manganese can be transported for long distance from hydrothermal vents, it has been revealed recently that iron can also travel relatively for long distance (Sander and Koschinsky 2011). Hence, ferromanganese oxides can be considered as chemical deposit that can be more or less produced related to the hydrothermal activities in marine environment. This book collected various scientific contributions related to hydrothermal activities at seafloor. From this aspect, ferromanganese oxide is important as one of consequences produced by such hydrothermal activities, which in turn can affect abundances and isotopic ratios of various trace elements in marine system.

To evaluate the effect of adsorption reactions on ferromanganese oxides, systematic understanding of adsorption of various trace elements is needed. The degree of adsorption reaction can be apparently designated by the adsorption distribution coefficient (= K_d) for an ion M as

$$K_d = [M_{ads}] / [M_{dis}], \quad (4.1)$$

where $[M_{ads}]$ and $[M_{dis}]$ are concentrations of adsorbed M in the solid phase and dissolved M in the aqueous phase, respectively. This manuscript aims to describe what is known for the adsorption reactions of trace elements with iron and manganese oxides to understand the effect on their concentrations and isotopic abundances in marine environment. In addition to the adsorption reaction, which is confined to the reaction at the solid-water interface in a narrow sense, incorporation into the iron and manganese oxides can be also important. The process can be called as coprecipitation that can be regulated by the size of the trace element to a larger degree than the adsorption reaction, since the coprecipitation incorporates the trace elements within the three dimensional structure of the precipitates (e.g., Cornell and Schwertmann 2003). However, we focus in this manuscript on the adsorption reaction which can be regarded as an elemental process even for the coprecipitation.

4.2 General Tendency for Cations

To discuss the affinity of trace elements for ferromanganese oxides, distribution ratios of trace elements in hydrogenetic ferromanganese oxides normalized by their concentrations in seawater are shown in Fig. 4.1 modified from Hein et al. (2000, 2003). The ratios for the hydrogenetic type can be important to discuss the solid-water distributions of various elements, since this type incorporates trace elements directly from those dissolved in seawater. This order of enrichment reflected in Fig. 4.1 can be explained by several factors such as

1. The ratio was generally higher for cations than those for anions. This fact is possibly caused by the fact that surface of the solid phase is negatively charged due to the dissociation of hydroxyl group at the surface of ferromanganese oxides, or in particular for manganese oxide (Langmuir 1997).
2. Cobalt is highly enriched due to the oxidation of its reductive form of Co(II) into its oxic species, Co(III) (Takahashi et al. 2007). Since Co(III) species is less soluble than Co(II) species, the enrichment of Co can be marked compared with other elements. Such oxidation is important reactions during the incorporation of trace elements into ferromanganese oxides due to the strong oxidation potential of manganese oxides. Similarly, the enrichment of Ce is much larger than those of other trivalent rare earth elements (REEs). This is also caused by the oxidation of Ce(III) into Ce(IV) by the oxidation potential of the manganese oxides, as shown by the large positive Ce anomalies in the hydrogenetic ferromanganese oxides (Takahashi et al. 2000; Takahashi et al. 2007). It is possible that oxidation of Tl(I) into Tl(III) can be also important for the enrichment of thallium into ferromanganese oxides (Peacock and Moon 2012).
3. If the oxidation reaction results in the increase of the solubility for an element, the degree of the enrichment can be lower such as for selenium and chromium by the oxidation of Se(IV) and Cr(III) into more soluble Se(VI) and Cr(VI). Hexavalent U, uranyl ion, forms anionic carbonate species in seawater (e.g., $UO_2(CO_3)_3^{4-}$) which inhibits interaction of uranyl ions with

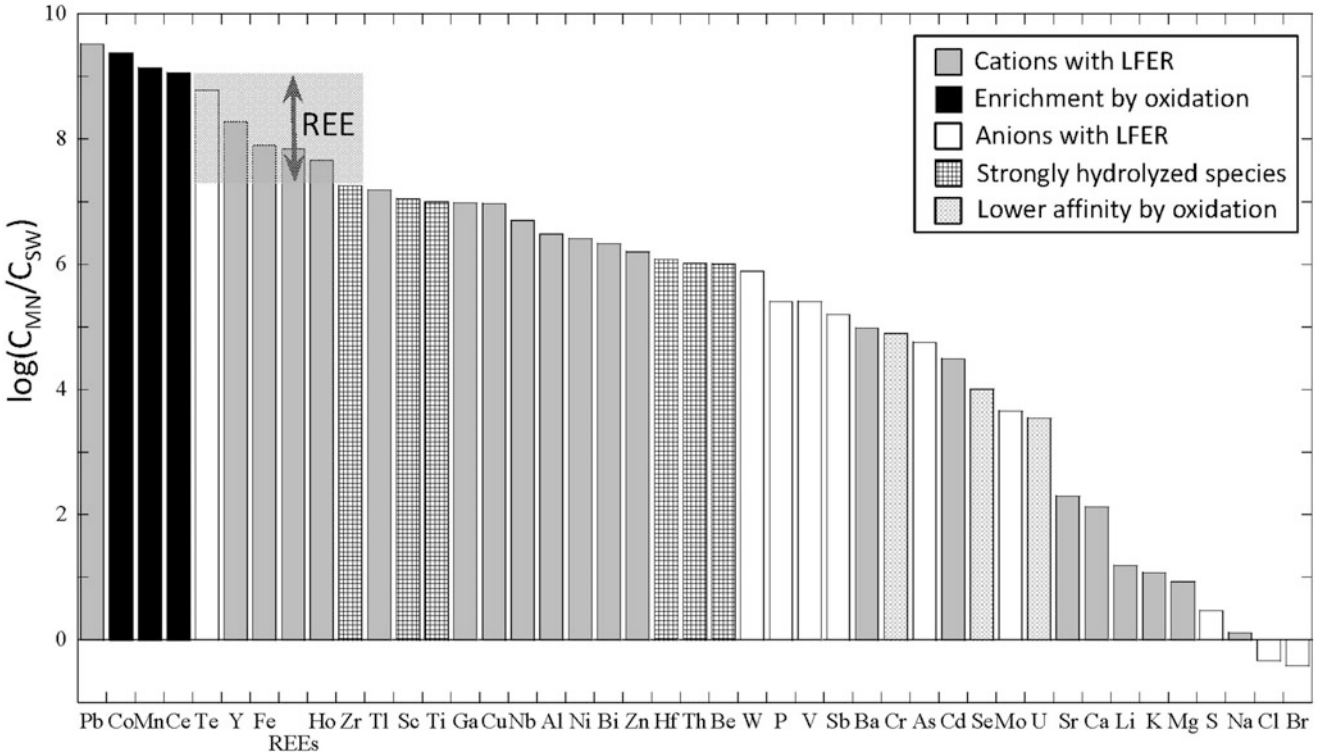

Fig. 4.1 Concentrations of various elements in hydrogenetic ferromanganese oxides (=C_{MN}) normalized by those in seawater (=C_{SW}) modified from Hein et al. (2000, 2003). Characteristic of incorporation of each element into hydrogenetic ferromanganese oxides is also indicated. *LFER* linear free energy relationship

ferromanganese oxides. Reduced form, U(IV), is highly insoluble, but U(IV) is readily oxidized in the presence of manganese oxides, which results in the lower abundance of U in ferromanganese oxides.

As indicated in (4.1), enrichment of cations is generally lager than that of anions (Fig. 4.1) and the cations (M^{z+}) are mainly bound to dissociated hydroxyl group at the surface of ferromanganese oxides ($\equiv S - O^-$) formulated by the reaction below:

$$\equiv S\text{-}O^- + M^{z+} <=> \equiv S\text{-}O\text{-}M^{(z-1)+} \qquad (4.2)$$

The reaction can be written by adsorption distribution coefficient K_d:

$$K_d = \left[\equiv S\text{-}O\text{-}M^{(z-1)+}\right]/([M^{z+}][\equiv S\text{-}O^-]) \qquad (4.3)$$

In particular, surface of manganese oxide is negatively charged, which leads to the preferential adsorption of cations.

Based on the relationship above, we can suggest relationships due to the analogous reaction of hydroxide formation of M^{z+}:

$$HO^- + M^{z+} <=> H\text{-}O\text{-}M^{(z-1)+} \qquad (4.4)$$

the stability of which is expressed by the stability constant of β_{OH} (Langmuir 1997),

$$\beta_{OH} = \left[MOH^{(z-1)+}\right]_{eq}/\left([M^{z+}]_{eq}[OH^-]_{eq}\right). \qquad (4.5)$$

In this case, it is expected that $\log K_d$ has a linear relationship against $\log\beta_{OH}$ as

$$\log K_d = a\log\beta_{OH} + b, \qquad (4.6)$$

where a and b are constants. Actually, K_d estimated by the solid-water distribution between ferromanganese oxides and seawater seems to be proportional to $\log\beta_{OH}$ as suggested by Li (1981, 1982) for cations (Fig. 4.2). This relationship is called as Linear Free Energy Relationship (LFER). As a result, the cation with larger stability constant with hydroxide is generally enriched into ferromanganese oxides. The ions with exceptionally different behavior is found in Fig. 4.2 for Co, Ce, Ba, and U, which can be interpreted by following reasons: (i) Co and Ce for the factor (4.2) as written above; (ii) Ba for the formation of insoluble sulfate (=barite) in the marine environment; (iii) UO_2^{2+} for its high stability of $UO_2(CO_3)_3^{4-}$ as dissolved species as indicated before.

To examine more clearly the LFER for cations, intrinsic surface complexation constant (= K_{int-2}: one of two intrinsic surface complexation constants, $K_{int\text{-}1}$and $K_{int\text{-}2}$, without electrostatic effect) experimentally obtained for ferrihydrite is discussed here due to the availability of a large amount of the data in Dzombak and Morel (1990), by which the

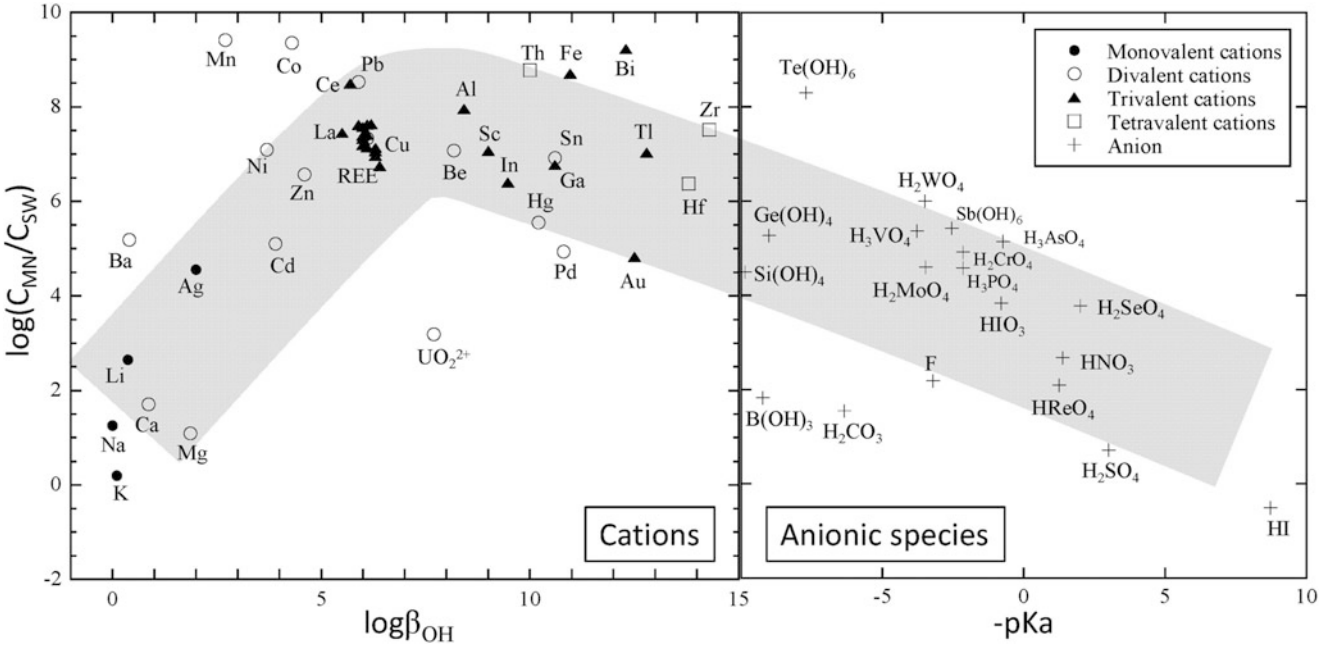

Fig. 4.2 Comparison of $\log(C_{MN}/C_{SW})$ to $\log\beta_{OH}$ for cations and –pKa of conjugate acids for anionic species

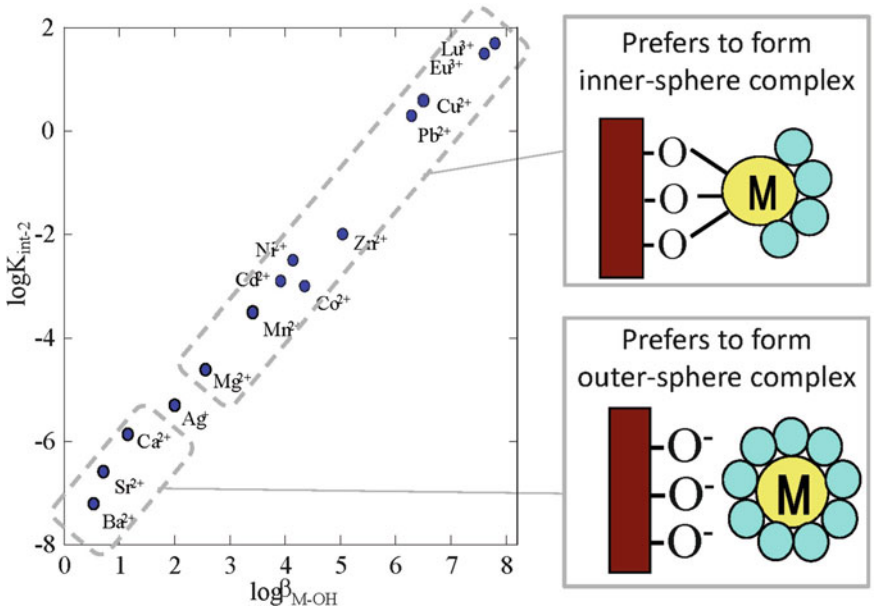

Fig. 4.3 The relationship between $\log K_{int\text{-}2}$ obtained by surface complex modeling for ferrihydrite (Dzombak and Morel 1990) and $\log\beta_{OH}$ for various cations, which is related to the preference to form either inner- or outer-sphere complex on ferrihydrite

relationship in Fig. 4.3 is depicted. The results again showed that the cation with larger $\log\beta_{OH}$ can have higher affinity for ferrihydrite. This tendency can explain high enrichment of Pb^{2+} and rare earth elements (REE) onto natural ferromanganese oxides. For hard cations (alkaline metal ions, alkaline earth metal ions, and rare earth ions), the systematics observed can be related to "ion potential" expressed by z/r, where z and r are charge and ionic radius of the ion. The higher the ion potential is, the larger the enrichment of the cation was observed. It has been previously suggested that enrichment of Pb is caused by the oxidation of Pb^{2+} into Pb^{4+}, but it is not likely based on the spectroscopic analyses (Takahashi et al. 2007). The high affinity for ferromanganese oxides coupled with high covalent characteristic of Pb^{2+} should be responsible for the large enrichment of Pb into the ferromanganese oxides.

Enrichment of Cu^{2+} in the natural ferromanganese nodules is not as large as that expected from $\log\beta_{OH}$ and $\log K_d$ values. This can be explained by preferential formation of organic complex for Cu^{2+} dissolved in seawater. The enrichment of Cu^{2+} for diagenetic ferromanganese nodule within sediment is generally larger than that in the

hydrogenetic ferromanganese nodule or crust growing at the surface of sediment or basement rock (Verlaan et al. 2004). The former type grows faster than hydrogenetic one by high flux of dissolved Mn^{2+} in the porewater in the sediment provided by the upward diffusion of dissolved Mn^{2+} in the sediment following the reduction of MnO_2 to Mn^{2+} (Dymond et al. 1984). The oxidation reaction by MnO_2 is accompanied with oxic degradation of organic matter in the deeper layer. On the other hand, the latter type (= hydrogenetic type) is formed by the direct precipitation of ferromanganese oxides in the water column. Thus, the preferential complexation of Cu^{2+} with organic matter and its degradation within the sediment is related to the large enrichment of Cu^{2+} in diagenetic ferromanganese oxides (Verlaan et al. 2004), but not the case for the hydrogenetic ferromanganese oxides expressed in Fig. 4.1.

Preferential formation of stable hydrolyzed species in the aqueous phase or even hydroxide precipitate can be a reason for the lower enrichment of high field strength elements such as Al^{3+}, Sc^{3+}, In^{3+}, Th^{4+}, Ga^{3+}, Fe^{3+}, Zr^{4+}, and Hf^{4+}. The $\log\beta_{OH}$ values for these ions are very large, but the degree of their enrichment is lower than the linear line expected from other cations in Fig. 4.2.

4.3 General Tendency for Anions

Similarly, anions can be attracted to the positively-charged surface of ferromanganese oxides ($\equiv$ S-OH_2^+) as shown by the following reaction including the anion written as L^{y-}:

$$\equiv \text{S-OH}_2^+ + \text{L}^{y-} <=> \equiv \text{S-L}^{(y-1)-} + \text{H}_2\text{O} \qquad (4.7)$$

with K_d as below:

$$K_d = \left[\equiv \text{S-L}^{(y-1)-}\right] / ([\equiv \text{S-OH}_2^+][\text{L}^{y-}]) \qquad (4.8)$$

For this reaction, we can expect another LFER based on the proton dissociation reaction known for many anions:

$$\text{H}^+ + \text{L}^{y-} <=> \text{HL}^{(y-1)-} \qquad (4.9)$$

In this case, we consider proton dissociation constant K_a (Langmuir 1997), by which we can write the equilibrium constant of the reaction above as $1/K_a$. Thus, LFER relationship for anions can be written as

$$\log K_d = a \log(1/K_a) + b = a\,pK_a + b \qquad (4.10)$$

This relationship was also suggested by Li (1981, 1982) as shown in right side of Fig. 4.2, where it is evident that the distribution ratio to ferromanganese oxide normalized to that in seawater is correlated to pKa_1 of the conjugate acids of the anions such as H_2SO_4 (conjugate acid) to HSO_4^- (anion) or HSO_4^- (conjugate acid) to SO_4^{2-} (anion). Equilibrium constant of the latter reaction between HSO_4^- and SO_4^{2-} is expressed by pKa_2, second proton dissociation constant of diprotic or triprotic acid. Similarly to Fig. 4.3, the comparison of pKa_2 value to $\log K_{int-2}$ defined in surface complexation model (Dzombak and Morel 1990) was also depicted for divalent oxyanions such as SO_4^{2-}, SeO_4^{2-}, MoO_4^{2-}, WO_4^{2-}, CrO_4^{2-}, SO_3^{2-}, SeO_3^{2-}, and SiO_3^{2-} (Fig. 4.4). In this figure, we can also see the clear correlation, showing that weaker acid that has higher affinity for proton (or larger pKa) can be more strongly adsorbed onto the surface of ferrihydrite.

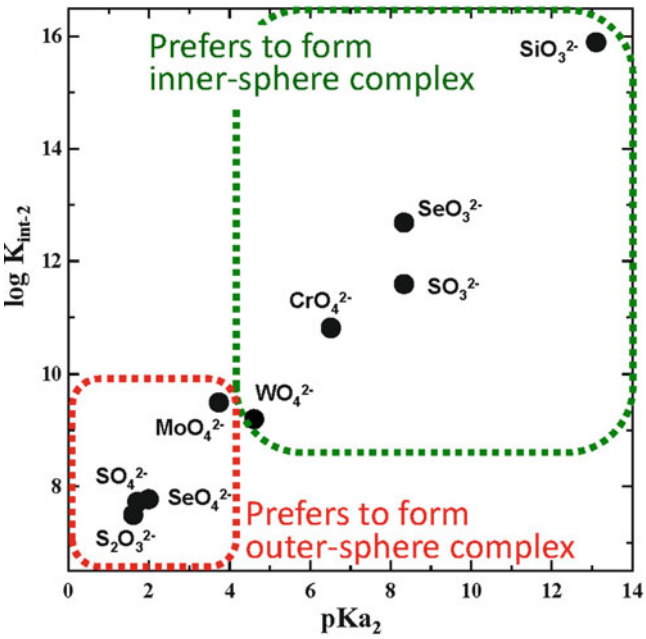

Fig. 4.4 The relationship between $\log K_{int-2}$ obtained by surface complex modeling for ferrihydrite (Dzombak and Morel 1990) and pKa_2 for conjugate acids of for various divalent oxyanions, which is related to the preference to form either inner- or outer-sphere complex on ferrihydrite

4.4 Relationship Between Distribution of Trace Elements and Their Local Structures at the Solid–Water Interface

The LFER suggests that the difference of distribution ratios of trace elements to ferromanganese oxides is primarily decided by the chemical affinity of each ion to the solid surface. If the affinity of one cation is larger for hydroxide ion (= larger β_{OH}) than the other cation, the ion also has a larger affinity to the proton-dissociated site on the solid phase. Similarly, if one conjugate acid (e.g., oxyacid like arsenate) has a larger affinity to proton (= larger pK_a) than the other, adsorption of the anion on the solid surface is relatively more stable in terms of the replacement of

hydroxyl groups attached to Fe^{3+} or Mn^{4+} by the anionic species. These species, including both cations and anions, which form direct bonding to the solid surface can be called as inner-sphere complex (Fig. 4.3). On the other hand, there are other species that can be retained on the solid surface without specific chemical bonding to the surface. In this case, the ion is electrostatically attracted to the surface without formation of chemical bonding (Fig. 4.3). The reaction can be called as ion-exchange reaction, where the species is known as outer-sphere complex.

For cations, for example, the difference of the affinity is also consistent with the local structure of cations adsorbed on the solid-water interface (Fig. 4.3). Based on the surface complex modeling on ferrihydrite or goethite, $Sr^{2+}$and Ca^{2+} mainly form outer-sphere complex to the surface (e.g., Cowan et al. 1991; Rahnemaie et al. 2006). On the other hand, Mg^{2+} having larger K_d value (Fig. 4.3) forms inner-sphere complex to goethite or ferrihydrite (e.g., Cowan et al. 1991; Rahnemaie et al. 2006). The difference of the structure, either outer-sphere or inner-sphere complexation, is directly linked to the stability of the surface complex: the K_d value of the ions forming outer-sphere complex is smaller than that forming inner-sphere complex.

The actual species of the surface complexes must be studied by any spectroscopic methods. Among various spectroscopic methods, extended X-ray absorption fine structure (EXAFS) is a unique technique (Bunker 2010), since (i) the method can be applied to almost all elements, (ii) the method is highly selective to the element without severe interference of other elements, (iii) the method is very sensitive that can be applied to trace elements at the solid-water interface, and (iv) the method is applicable in the presence of water in the system without necessity of drying upon the measurement. The EXAFS can give distance (R) of center atom to the neighboring atoms with coordination number (CN) of the neighboring atom. In the adsorption system, EXAFS can reveal the type of the surface complex based on the R with CN for first and second neighboring atoms, as exemplified by La^{3+} adsorbed on ferrihydrite (Fig. 4.5; Nakada et al. 2013). If the populations of inner- and outer- sphere complexes are rather similar, it is sometimes difficult to determine the CN of the second neighboring atom, or Fe in this case. More importantly, however, the presence of the peak of the second neighboring atom (e.g., La-Fe in Fig. 4.5) is important, which can be strong evidence of the formation of inner-sphere complex, or more precisely the dominance of the inner-sphere complex for the ion.

Taking account of the background of the EXAFS spectroscopy, let us consider the structure, whether inner- or outer-sphere complex are important for the cations and anions related to Figs. 4.3 and 4.4. As for cations, Sr^{2+} forms outer-sphere complex on ferrihydrite (Langley et al. 2009). Although spectroscopic information on the

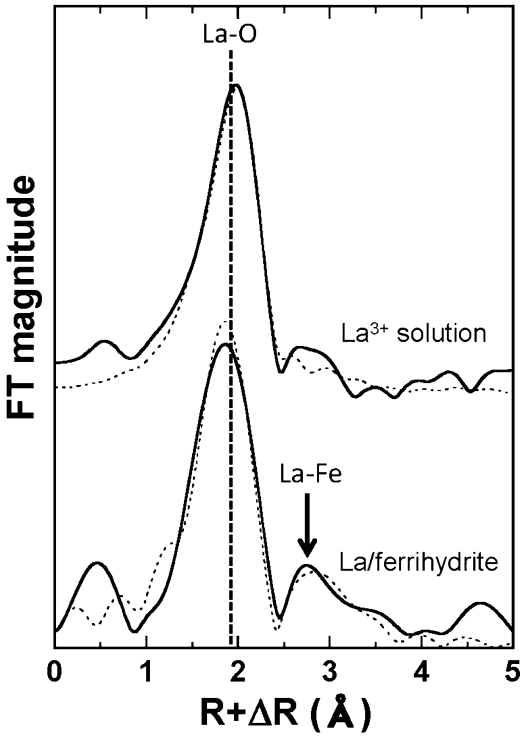

Fig. 4.5 Lanthanum K-edge EXAFS in R-space as an example of spectrum for cations adsorbed on ferrihydrite

surface complexes of Ca^{2+}, Ag^{+}, and Mg^{2+} is not available, inner-sphere complex on ferrihydrite has been observed for Cd^{2+}adsorbed on iron oxides (e.g., Spadini et al. 1994). These facts both from modeling and spectroscopic results illustrate that the chemical affinity expressed by $\log\beta_{OH}$ decides whether the ion forms inner- or outer-sphere complex on ferrihydrite. In this discussion, it must be noted that all ions more or less form both inner- and outer-sphere complexes on the solid phase. However, the ratio of the inner- to outer- sphere complexes on certain solid phase can follow the order shown in Fig. 4.3.

Similar tendency has been suggested for oxyanions based on the structure of surface complexes of oxyanions on ferrihydrite recently revealed by Harada and Takahashi (2008) and Kashiwabara et al. (2011, 2013). Harada and Takahashi (2008) studied adsorbed species of selenate, selenite, tellurite, and tellurate on ferrihydrite. They concluded that selenate forms outer-sphere complex on ferrihydrite, whereas selenite, tellurite, and tellurate form inner-sphere complex based on the EXAFS analyses. Kashiwabara et al. (2011, 2013) showed that molybdate and tungstate form outer- and inner-sphere complexes on ferrihydrite, respectively. In Fig. 4.4, it is also evident that the affinity to the solid surface ($\log K_{int\text{-}2}$) is larger for those ions forming inner-sphere complex (selenite, tellurite, and tellurate) than that taking outer-sphere complex (selenate and molybdate). However, the tendency is somewhat opposite between molybdate and tungstate. Hence, more details

for oxyanions will be given below including additional spectroscopic data of chromate adsorption on ferrihydrite, since chromium is a congener of molybdenum and tungsten.

4.5 Adsorption of Chromate: Additional Spectroscopic Data

To obtain more structural information on the adsorption of divalent oxyanions on ferrihydrite, EXAFS spectrum of chromate was also obtained in this study. As seen in Fig. 4.4, information of chromate can be important, since the ion is located between tungstate and selenate discussed above in terms of the pKa_2 value. For this purpose, chromium K-edge (5.989 keV) EXAFS was mainly measured at beamline BL-12C of KEK Photon Factory (Tsukuba, Japan) with a Si(111) double–crystal monochromator and two mirrors. The measurement was carried out at room temperature under ambient conditions. The XAFS spectra of the reference compounds were collected in transmission mode, whereas those of the experimental samples were obtained in the fluorescence mode. In the latter mode, the sample was positioned at 45° with respect to the incident, while a 19–element germanium semiconductor detector (Canberra, USA) placed at 90° to the incident beam. Multiple scans were taken for low Cr concentration samples to obtain sufficiently high signal/noise ratio for EXAFS simulations. Repeated scan gave identical spectra, which assures the minimal alteration of the sample by the incident X-ray.

As for the sample of chromate adsorbed on ferrihydrite, adsorption experiments were carried out using 20 mg of ferrihydrite and 10 mL chromate solution. Adsorption envelops under different ionic strengths were obtained at various pH at an initial chromate concentration of ca. 300 μM. Ionic strength was adjusted to 0.010 M or 0.70 M by $NaNO_3$ at each pH. The pH was adjusted by a 0.10 M NaOH or 0.10 M HNO_3 solution to desired values. After 24 h of equilibration at 25 °C, samples were filtered using 0.20 μm membrane filter. The filtrates were diluted adequately, and concentrations of chromate were measured by ICP-MS to obtain the amount of chromate adsorbed on ferrihydrite.

The adsorption envelopes for chromate on ferrihydrite are shown in Fig. 4.6. The result shows that the adsorption of chromate depends on pH, where the maximum chromate adsorption was found at pH 5. The pH dependence of adsorption of oxyanions is often related to the charges loaded on the solid phase and proton dissociation behavior of oxyacids. As for ferrihydrite employed as solid phase in this study, negative charges increase with the increase in pH (Langmuir 1997), where the adsorption amount of anion monotonously decreases if the form of the anion does not change. The maximum adsorption at pH 5 reflects the influence of acid dissociation behavior of chromic acid:

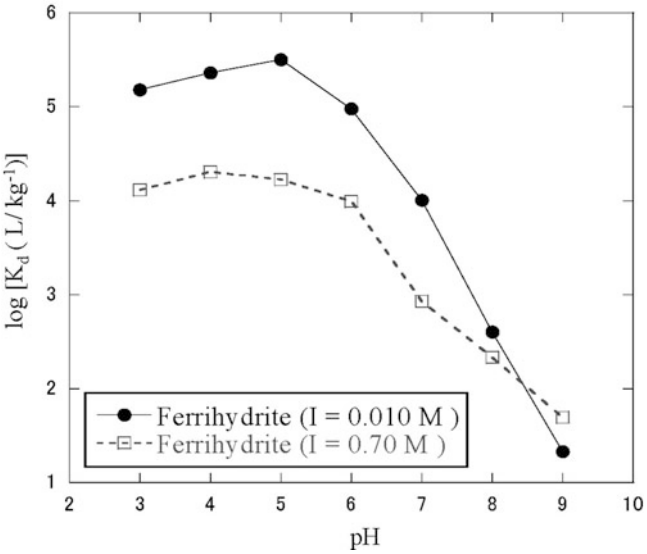

Fig. 4.6 Adsorption envelopes for chromate on ferrihydrite at I = 0.010 and 0.70 M

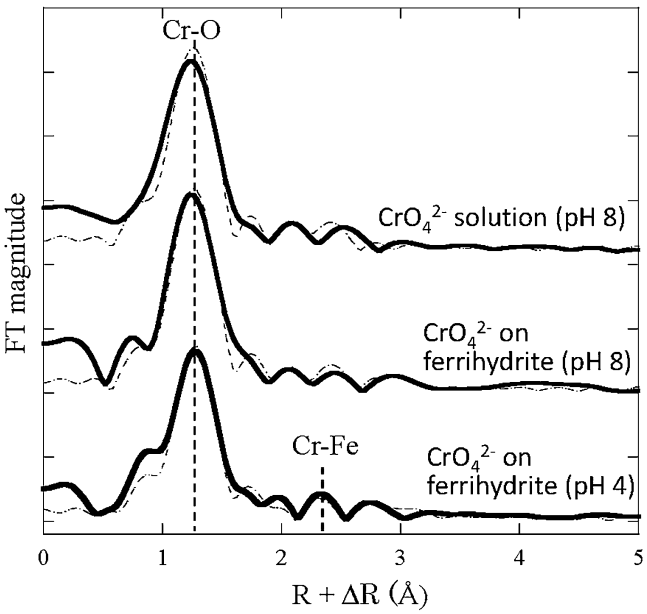

Fig. 4.7 Chromium K-edge EXAFS in R space for chromate solution and chromate adsorbed on ferrihydrite

the increase of K_d up to pH 5 was caused by its larger pKa_2 value for second dissociation ($pKa_2 = 6.51$). As the concentration of ionic strength ($NaNO_3$) increased from 0.010 to 0.70 M, the chromate adsorption on ferrihydrite obviously decreased (Fig. 4.6). The decrease of K_d by the increase of ionic strength suggests the formation of outer-sphere complex for chromate adsorbed on ferrihydrite (Hayes et al. 1988).

Figure 4.7 shows Cr K–edge EXAFS spectra, or their radial structural functions (RSF: phase shift not corrected)

Table 4.1 Structural parameters of chromate adsorbed on ferrihydrite and solution obtained by curve fitting of EXAFS spectra

Sample	Shell	CN	R (Å)	ΔE^o (eV)	σ^2	R factor (%)
Cr (VI)-solution (pH 8)	Cr-O	3.5	1.66	−2.56	0.003[a]	3.80
Ferrihydrite (pH 4)	Cr-O	3.3	1.66	1.63	0.003[a]	3.56
	Cr-Fe	0.40	3.33		0.002[a]	
Ferrihydrite (pH 8)	Cr-O	3.3	1.66	−2.38	0.003[a]	3.85

[a]Fixed value in the fitting process

for the chromate solution and chromate adsorbed on ferrihydrite. The adsorption samples on ferrihydrite at pH 4 and 8 were measured, where we found that all the spectra in Fig. 4.7 were almost the same. However, spectra of solution and adsorbed sample were slightly different. Although the position of the first shell (R = ca. 1.6 Å) are similar between solution and adsorption samples, a second shell at R = 2.8 Å was observed at pH 4. However, the peak is not evident at pH 8 and for chromate solution (Fig. 4.7).

The CN, interatomic distances (R), and Debye–Waller factors (σ^2) obtained from the curve–fitting analysis are summarized in Table 4.1. The parameters obtained for the sample at pH 8 was almost identical to those of the solution sample (Table 4.1). Although the spectrum for the adsorption sample at pH 4 was fitted well with Cr–Fe assigned as the second shell, the CN value was very small (ca. 0.4). These facts suggested that chromate is adsorbed on ferrihydrite mainly as outer–sphere complex with contribution of a small amount of inner–sphere complex at lower pH. This EXAFS data are consistent with what was estimated by the dependence of K_d on ionic strength.

4.6 Two pKa Model

The previous section has shown that chromate is adsorbed on ferrihydrite mainly as outer–sphere complex. In our previous studies, it was found that molybdate and tungstate are adsorbed on ferrihydrite as outer–sphere and inner–sphere complexes, respectively (Kashiwabara et al. 2011, 2013). In spite of possible similar chemical characteristics as congeners, chromate, molybdate, and tungstate are adsorbed on ferrihydrite by different attachment modes (i.e., inner– or outer– sphere). The attachment mode in turn is closely related to the solid–water distribution of the oxyanions as seen from the adsorption of chromate, molybdate, and tungstate (Figs. 4.1 and 4.4): tungstate which forms inner–sphere complex is largely distributed to the solid phase, but chromate and molybdate forming outer–sphere complexes are soluble due to the smaller affinity to the solid phase.

As suggested in Sect. 4.4, LFER has been utilized, in which equilibrium constant such as $\log K_d$ is proportional to that of pK_a of conjugate acids of oxyanions such as $HMoO_4^-$ for molybdate (MO_4^{2-}). In this context, Dzombak and Morel (1990) showed that the logarithm of intrinsic surface complex constant $K_{int\text{-}2}$ is linearly correlated with that of pKa_2 of such oxyacids (Fig. 4.4). The acid with low pK_a (= strong acid) prefers to release proton due to the high stability of hydration of the conjugate oxyanions, which results in the formation of outer–sphere complex as indicated above and vice versa. Hence, we compared pK_{a1} and pK_{a2} for various acids of divalent oxyanions such as Group A (SeO_4^{2-}, SO_4^{2-}, CrO_4^{2-}, MoO_4^{2-}) and Group B (WO_4^{2-}, TeO_3^{2-}, SeO_3^{2-}, $TeO_2(OH)_4^{2-}$, in Fig. 4.4. The former group prefers to form outer–sphere complex on ferrihydrite (Bigham et al. 1990; Harada and Takahashi 2008; Kashiwabara et al. 2011), while the latter inner–sphere complex (Harada and Takahashi 2008; Waychunas et al. 1993; Pokrovski et al. 2003; Kashiwabara et al. 2013).

As shown in Fig. 4.8, pK_{a2} rather than pK_{a1} value is correlated with the preference of inner–sphere complex. In the case of pK_{a1}, pK_{a1} values of conjugate acids of TeO_3^{2-} and SeO_3^{2-} are relatively low, but these anions mainly form inner–sphere complexes to ferrihydrite. On the other hand, pK_{a2} value can predict the formation of inner–sphere complex: oxyanions with pK_{a2} larger than WO_4^{2-} prefer to form inner–sphere complex (Fig. 4.4). However, the chromate which forms outer–sphere complex with larger pK_{a2} is exceptional in this relationship. Instead of pK_{a1} or pK_{a2}, we here propose that the average of pKa_1 and $pK_{a2}\left(= p\overline{K}_a = (pK_{a1} + pK_{a2})/2\right)$ can be more useful to predict the inner–sphere and outer–sphere complexation: conjugate anions of oxyacids having $p\overline{K}_a$ larger than H_2WO_4 prefer to form inner–sphere complex on ferrihydrite.

Inclusion of both pK_{a1} and pK_{a2} for this criterion is reasonable considering the structure of surface complexes. If these oxyanions such as chromate, molybdate, and tungstate form inner–sphere complexes, it is most likely that they form bidentate complex to the ferrihydrite surfaces via. two oxygens from the center atom as shown for molybdate and tungstate. The better correlation between the outer–/inner–sphere complex and $p\overline{K}_a$ rather than pK_{a1} and pK_{a2} means that both of two –OH groups of the oxyanion are responsible for the stability of its surface complex to the ferrihydrite surface. This fact is consistent with the structural data that they form bidentate surface complex to ferrihydrite: these divalent oxyanions are bound to the ferrihydrite surface via. two oxygens, if they form inner-sphere complex (e.g.,

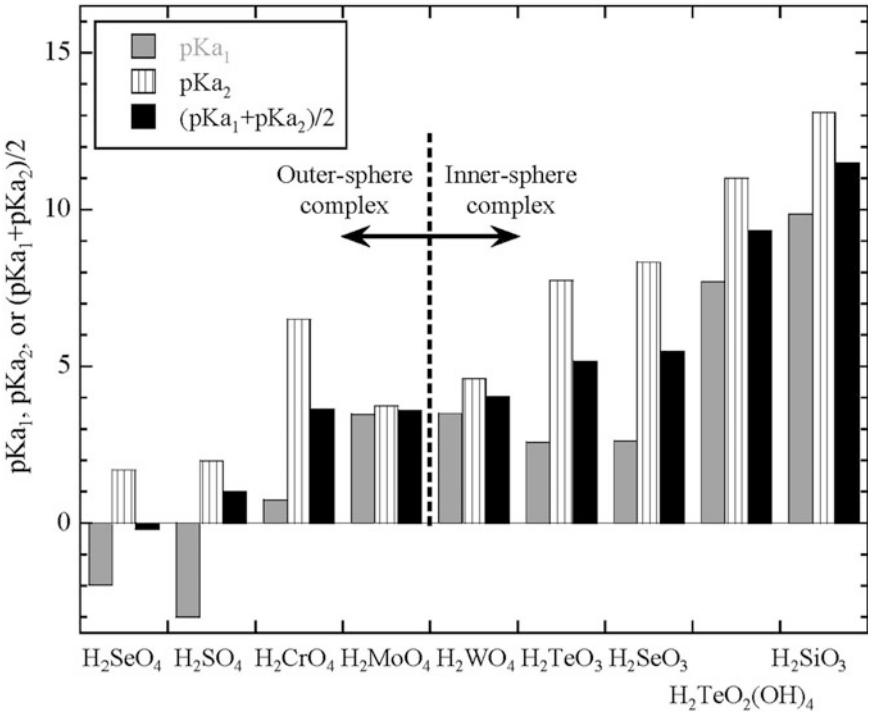

Fig. 4.8 The pKa values and attachment modes on ferrihydrite of various oxyanions

Kashiwabara et al. 2011; Kashiwabara et al. 2013). Thus, the chemical effect of both proton dissociation groups must be taken into account to evaluate the stability of the surface complex reflected in pKa_1 and pKa_2. Hence, $p\overline{K}_a = (pK_{a\,1} + pK_{a\,2})/2$ is shown to be useful to predict attachment mode of oxyanions to ferrihydrite.

4.7 Conclusions and Implications

In this review, it was clear that attachment mode of the surface complex is closely related to the solid-water distribution or the degree of enrichment to ferromanganese oxides for various elements. Moreover, attachment mode of the surface complex governs the isotopic fractionation of trace elements during the adsorption on solid phases indicated in Sect. 4.1. It has been indicated that adsorption reaction with outer-sphere complexations does not induce isotopic fractionation, possibly because the local structure of the element does not change by the adsorption reaction. However, formation of inner-sphere complex during adsorption can cause isotopic fractionation. For example, it has been indicated that molybdenum isotope can be fractionated by its adsorption on manganese oxides by the inner-sphere complexation, but not on ferrihydrite adsorbing molybdate ion as outer-sphere complex of hydrated ion (Kashiwabara et al. 2011). Similarly, adsorption of chromate does not cause large isotopic fractionation due to the outer-sphere complexation for the adsorption.

On the other hand, the adsorption structure can be systematically interpreted by the pKa value of conjugate acid and $\log\beta_{OH}$ for anions and cations, respectively. Hence, such systematic understanding of the adsorption reaction in terms of pKa and $\log\beta_{OH}$ enables us to predict the distribution and isotopic fractionation of various elements. Considering that the distribution and isotopic fractionation are very important for the understanding the behavior in marine environment, enrichment mechanism, and development of isotopic ratio as paleoenvironmental tool for various elements, systematic interpretation described in this study is useful in various geochemical aspects.

Acknowledgements This research was supported by a grant-in-aid for scientific research from the Ministry of Education, Science, Sports, and Culture of Japan including "TAIGA" project accepted as a Scientific Research on Innovative Areas. This work has been performed with the approval of JASRI (Proposal No. 2013A1177) and KEK (Proposal No. 2009G585 and 2011G635).

References

Bigham JM, Schwertmann U, Carlson L, Murad E (1990) A poorly crystallized oxyhydroxy sulfate of iron formed by bacterial oxidation of Fe(II) in acid mine waters. Geochim Cosmochim Acta 54:2743–2758

Bunker G (2010) Introduction to XAFS: a practical guide to X-ray absorption 0fine structure spectroscopy. Cambridge University Press, London

Cornell RM, Schwertmann U (2003) The iron oxides. Wiley-VCH, Weinheim

Cowan CE, Zachara JM, Resch CT (1991) Cadmium adsorption on iron-oxides in the presence of alkaline-earth elements. Environ Sci Technol 25:437–446. doi:10.1021/es00015a009

Dymond J, Lyle M, Finey B, Piper DZ, Murphy K, Conard R, Pisias N (1984) Ferromanganese nodules from MANOP Sites H, S, and R—control of mineralogical and chemical composition by multiple accretionary processes. Geochim Cosmochim Acta 48:931–949

Dzombak DA, Morel FMM (1990) Surface complexation modeling: hydrous ferric oxide. Wiley, New York, p 393

Elderfield H, Schultz A (1996) Mid-ocean ridge hydrothermal fluxes and the chemical composition of the ocean. Ann Rev Earth Planet Sci 24:191–224. doi:10.1146/annurev.earth.24.1.191

Harada T, Takahashi Y (2008) Origin of the difference in the distribution behavior of tellurium and selenium in a soil–water system. Geochim Cosmochim Acta 72:1281–1294

Hayes KF, Papelis C, Leckie LO (1988) Modeling ionic strength effects on anion adsorption at hydrous oxides/solution interfaces. J Colloid Interface Sci 125:717–726

Hein JR, Koschinsky A, Bau M, Manheim FT, Kang J-K, Roberts L (2000) Cobalt-rich ferromanganese crusts in the Pacific. In: Cronan DS (ed) Handbook of marine mineral deposits. CRC, Boca Raton, pp 239–279

Hein JR, Koschinsky A, Halliday AN (2003) Global occurrence of tellurium-rich ferromanganese crusts and a model for the enrichment of tellurium. Geochim Cosmochim Acta 67:1117–1127

Kashiwabara T, Takahashi Y, Tanimizu M, Usui A (2011) Molecular scale mechanisms of distribution and isotopic fractionation of molybdenum between seawater and ferromanganese oxides. Geochim Cosmochim Acta 75:5762–5784

Kashiwabara T, Takahashi Y, Matthew AM, Uruga T, Tanida H, Terada Y, Usui A (2013) Tungsten species in natural ferromanganese oxides related to its different behavior in oxic ocean from molybdenum. Geochim Cosmochim Acta 75:5762–5784

Langley S, Gault AG, Ibrahim A, Takahashi Y, Renaud R, Fortin D, Clark ID, Ferris FG (2009) Sorption of strontium onto bacteriogenic iron oxides. Environ Sci Technol 43:1008–1014. doi:10.1021/es802027f

Langmuir D (1997) Aqueous environmental geochemistry. Prentice Hall, Upple Saddle River

Li Y-H (1981) Ultimate removal mechanisms of elements from the ocean. Geochim Cosmochim Acta 45:1659–1664

Li Y-H (1982) Ultimate removal mechanisms of elements from the ocean (reply to a comment by M. Whitfield and D. R. Turner). Geochim Cosmochim Acta 46:1993–1995

Lyons TW, Anbar AD, Severmann S, Scott C, Gill BC (2009) Tracking Euxinia in the ancient ocean: a multiproxy perspective and proterozoic case study. Annu Rev Earth Planet Sci 37:507–534

Nakada R, Tanimizu M, Takahashi Y (2013) Difference in the stable isotopic fractionations of Ce, Nd, and Sm during adsorption on iron and manganese oxides and its interpretation based on their local structures. Geochim Cosmochim Acta 121:105–119

Peacock CL, Moon EM (2012) Oxidative scavenging of thallium by birnessite: explanation for thallium enrichment and stable isotope fractionation in marine ferromanganese precipitates. Geochim Cosmochim Acta 84:297–313

Pokrovski GS, Schott J, Farges F, Hazemann JL (2003) Iron (III)–silica interactions in aqueous solution: insights from X-ray absorption fine structure spectroscopy. Geochim Cosmochim Acta 67:3559–3573

Rahnemaie R, Hiemstra T, van Riemsdijk WH (2006) Inner- and outer-sphere complexation of ions at the goethite-solution interface J Colloid Interface Sci 297:379–388

Sander SG, Koschinsky A (2011) Metal flux from hydrothermal vents increased by organic complexation. Nat Geosci 4:145–150

Spadini L, Manceau A, Schindler PW, Charlet L (1994) Structure and stability of Cd2+ surface complexes on ferric oxides: 1. Results from EXAFS spectroscopy. J Colloid Interface Sci 168:73–86

Takahashi Y, Shimizu H, Usui A, Kagi H, Nomura M (2000) Direct observation of tetravalent Cerium in ferromanganese nodules and crusts by X-ray absorption near-edge structure (XANES). Geochim Cosmochim Acta 64:2929–2935

Takahashi Y, Manceau A, Geoffroy N, Marcus MA, Usui A (2007) Chemical and structural control of the partitioning of Co, Ce, and Pb in marine ferromanganese oxides. Geochim Cosmochim Acta 71:984–1008

Verlaan PA, Cronan DS, Morgan CL (2004) A comparative analysis of compositional variations in and between marine ferromanganese nodules and crusts in the South Pacific and their environmental controls. Prog Oceanogr 63:125–158

Waychunas GA, Rea BA, Fuller CC, Davis JA (1993) Surface–chemistry of ferrihydrite: Part 1. EXAFS studies of the geometry of coprecipitated and adsorbed arsenate. Geochim Cosmochim Acta 57:2251–2269